VOL. 11, NO. 6, MARCH 2016 ISSN 1819-6608
ARPN Journal of Engineering and Applied Sciences

www.arpnjournals.com

REPRESENTATION OF HUMAN GAIT TRAJECTORY THROUGH TEMPOROSPATIAL IMAGE MODELLING

Md. Akhtaruzzaman, Amir A. Shafie and Md. Raisuddin Khan
Department of Mechatronics Engineering, Kulliyyah of Engineering, International Islamic University Malaysia, Kuala Lumpur, Malaysia
E-Mail: akhter900@gmail.com

ABSTRACT

Marker-based 2D temporospatial image modelling is a common strategy in characterizing human gait where Channel filtering, Threshold imaging, and Line feel algorithm are normally used in foreground segmentation targeting human lower limbs of a particular image frame. This paper presents Temporospatial Image Modelling approach in presenting segmented objects with spatiotemporal view by reflecting various poses of lower limbs for forward walking. Lower limbs joint movement characteristics and angle variations are also presented in this paper where pre-assigned marker-points are modelled in tracking the motion trajectories. Results show various patterns of motion trajectories and angle variations for Hip, Knee, Ankle, Heel, and Toe of lower limbs through observing the variations of times, locations, and spatiotemporal representations. The results also characterize that the Swing and Stance phases of a gait cycle are about 40% and 60% of a gait cycle respectively.

Keywords: image processing, spatiotemporal image, walking gait, gait analysis, temporospatial modelling.

INTRODUCTION

Image base gait characterization and classification strategies can be studied based on three dimensional (3D) approach where multi-camera module is necessary [1] or two dimensional (2D) approach where only a single stationary camera is used [2]. Extraction of high-level features from continuous image, usually depend on marker based motion capture strategy [3]. Markers could be active or passive which are attached at the point of interests of human body [4]. On the other hand, marker-less motion analysis is one of the promising alternatives in gait analysis [5].

Multi camera based marker less system is presented by B. Rosenhahn *et al.* [6] where silhouette based human motion estimation for upper limbs is experimented. O. Rashid *et al.* [7] experimented on 2D image sequence and depth image sequence in object segmentation and computed statistical and geometrical feature vectors in posture recognition based on Support Vector Machines (SVM). Optical marker based body motion analysis is presented by R. Tranberg [8]. In this study skin markers were applied to analyze soft tissue motion where stereo image of internal structure of lower limbs are constructed using radiostereometry.

Foreground segmentation for moving object extraction is the pre-step in human detection and also in human gait classification. F. Hafiz *et al.* [9] used Gaussian Mixture Modeling (GMM) in segmenting foreground to detect moving subjects. Spatiotemporal representation of image sequence is another effective way for gait recognition, and motion analysis as presented by M. Jeevan *et al.* [10].

Identification of joint positions, motion trajectories, and angle variations during walking are rally challenging. 3D analysis involves complex setup of experimental environment with multiple cameras places in multiple angles from targeted subject location. Moreover, processing complication increases in modelling 3D view of the subject. Marker-less analysis increases computational difficulties and decreases accuracy in selecting interest points. This paper presents marker-based 2D analysis technique that reduces system complexities, computational overheads and ensures accuracy in selecting interest point positions. The objective of this study is to model 2D spatiotemporal image of human walking, marker based analysis to extract motion trajectories, and characterization of gait. Outcomes of the experiment reflects spatiotemporal representation of walking gait, feature identifications and presentations of motion trajectories with respect to times, locations, and spatiotemporal view. Results presented in this paper are based on image sequence of single person walking gait.

ORGANIZATION OF THE PAPER

Firstly, experimental setup and segmentation strategy are introduced. Secondly, spatiotemporal image modelling algorithm is presented. Thirdly, marker based feature extraction procedures are explicated. Fourthly, output results are scrutinized. Finally, concluding remarks.

EXPERIMENTAL SETUP

Figure-1 represents a particular image frame of a video stream where Figure-1(a) is original image with resolution $[(width\ (w) * height(h)\ ) = (1280 * 720)]$ or $\approx 0.9\ Mega - pixels\ (Mp)$. Figure-1(b) is cropped frame with resolution $(1010 * 471)$ or $\approx 0.4\ Mp$. Video stream is taken using Samsung Galaxy Note II (GT-N7100) $8\ Mp$ camera with same resolution settings as presented in Figure-1(a).

VOL. 11, NO. 6, MARCH 2016 ISSN 1819-6608
ARPN Journal of Engineering and Applied Sciences

www.arpnjournals.com

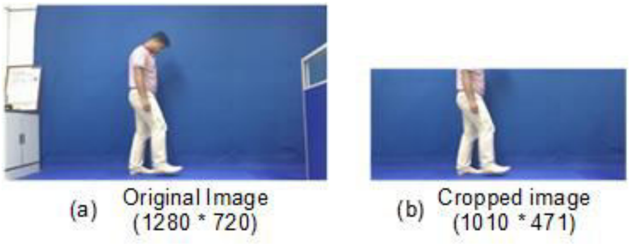

Figure-1. (a) Original image frame, and (b) Cropped image frame for processing.

Because of light intensity, blue background is not evenly distributed and has some gradient features. Variations of the gradient feature are also appears depending on various positions of foreground. Moreover, shadows of the focused subject changes luminosity of some particular part of image frame. Each image frame also contains black regions most commonly in between lower limbs.

Foreground segmentation is prerequisite in temporospatial image modelling. To perform segmentation process, several strategies are applied in this experiment; firstly, optimal channel selection among Red, Green, and Blue channels; secondly, greyscale conversion; thirdly, threshold imaging; and finally, applying line-fill algorithm in smoothing foreground region of threshold image. The procedure block diagram is presented in Figure-2.

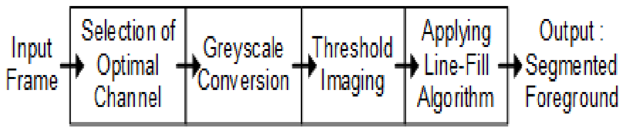

Figure-2. Procedure block diagram of foreground segmentation.

TEMPOROSPATIAL IMAGE MODELLING

Temporospatial representation is the reflection of space and time both in a single dimension that helps to understand motion behaviour pattern at a glance. Figure-3 presents block diagram in modelling temporospatial image. First of all, segmentation algorithm is applied for each frame of image sequence without losing the position information of each foreground. Then transparency level is set to 10% for each segmented object. Finally, all the foregrounds are merged together based on the position information and placed on original empty background where background transparency level remains 100%. Result of the procedure presents a temporospatial image of human forward walking.

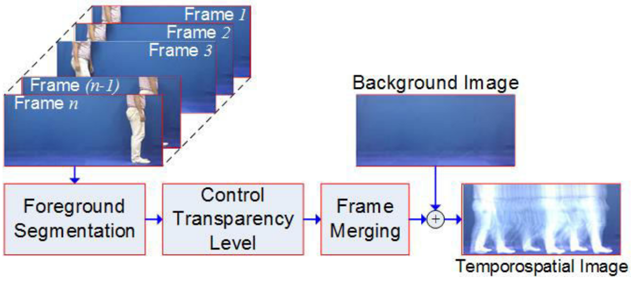

Figure-3. Block diagram of temporospatial imaging and representation of image stream.

MARKER POSITION IDENTIFICATION AND FEATURE EXTRACTION

Procedure is subdivided into three steps; First: five sticker-markers at Hip, Knee, Ankle, Heel, and Toe positions are attached as shown in Figure-4(a); Second: marker corrections with three different colours (Red, $RGB = (255, 0, 0)$, for Hip, Knee, and Ankle joints; Green, $RGB = (0, 255, 0)$, for Heel; and Cyan, $RGB = (0, 255, 255)$, for Toe position) are performed as shown in Figure-4(b); Third: identification of joint positions using colour markers and all the position information of each joint are accumulated in a series. At each time when a marker is identified, centre position is calculated considering joint position and at the same time marker is erased to avoid repetition as presented in Figure-4(c).

Marker position identification process can be represented by Equation. (1), where f indicates image frames ($f = 1,2,3, \dots, n$). Hp, Kn, An, Hl, and To present position array of five markers for all image frames. R_{Hp}, R_{Kn}, R_{An}, G_{Hl}, and C_{To} are expressing colours of five marker points. Function, $MarkerPoint(\bullet)$, process the five markers and returns five position values. M_{mask}, illustrates marker mask to erase a processed marker.

$$E_{f=1}^{f=n}\left([Hp, Kn, An, Hl, To]_f; \left(R_{Hp}, R_{Kn}, R_{An}, G_{Hl}, C_{To}\right)_f\right) = E_{f=1}^{f=n}\left(MarkerPoint(R_{Hp}, R_{Kn}, R_{An}, G_{Hl}, C_{To})_f; (M_{mask})\right) \quad (1)$$

VOL. 11, NO. 6, MARCH 2016 ISSN 1819-6608
ARPN Journal of Engineering and Applied Sciences

www.arpnjournals.com

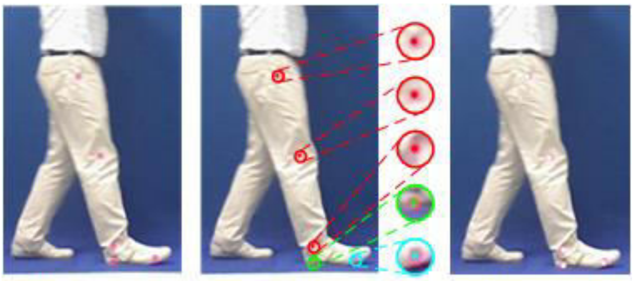

(a) Image of a Gait pose with sticker markers.
(b) Gait pose with digital color markers (corrections).
(c) Image of a Gait pose after removing markers.

Figure-4. (a) Demonstration of assigning sticker-markers, (b) Marker corrections and assigning colour for each marker, and (c) Removing each marker after applying marker point detection procedure.

During marker correction, five circular marker points with diameter (d) of 7 pixels are applied. Figure-5 presents distribution, indexing, and index linearization of pixels of a marker model. A marker is considered as identified if any of the boundary point is detected during linear search. As markers are circular, the first pixel is detected as $(x-1, y-3)$ where (x, y) is the center of the marker. In practical case, pixels of a circular marker may not be evenly distributed. So, a marker mask is designed with diameter, $d = 11\ pixels$ to erase detected marker.

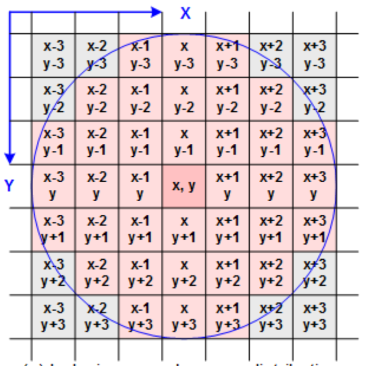

(a) Indexing a marker area distribution.

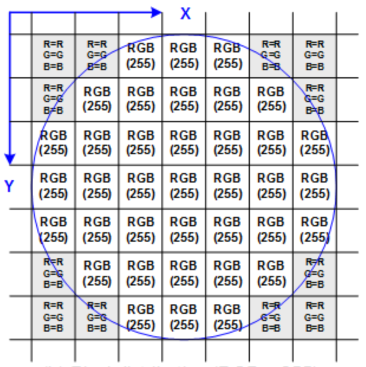

(b) Pixel distribution (RGB = 255).

(c) Linearization of marker pixel index.

	σ_x	σ_y
1	-1	-3
2	0	-3
3	1	-3
4	-2	-2
5	-1	-2
6	0	-2
7	1	-2
8	2	-2
9	-3	-1
10	-2	-1
11	-1	-1
12	0	-1
13	1	-1
14	2	-1
15	3	-1
16	-3	0
17	-2	0
18	-1	0
19	0	0
20	1	0
21	2	0
22	3	0
23	-3	1
24	-2	1
25	-1	1
26	0	1
27	1	1
28	2	1
29	3	1
30	-2	2
31	-1	2
32	0	2
33	1	2
34	2	2
35	-1	3
36	0	3
37	1	3

Figure-5. Indexing and pixels distribution of marker with linear representation of pixel index factor.

Erasing a marker can be presented by Equation. (2) where σ_x, and σ_y indicate linearized index factors for $i = 1,2,3,\ldots,n$; here $n = 37$. M presents marker pixel distribution with $R_{(x,y)}$, $G_{(x,y)}$, and $B_{(x,y)}$ color properties. Number 255 is representing highest colour value of each marker pixel. Combining all the procedures, final algorithm block diagram for feature extraction from walking image sequence is presented in Figure-6.

$$E_{i=1}^{i=n}\left(M\left(R_{((x+\sigma_{x_i}),(y+\sigma_{y_i}))}, G_{((x+\sigma_{x_i}),(y+\sigma_{y_i}))}, B_{((x+\sigma_{x_i}),(y+\sigma_{y_i}))}\right)\right) = 255 \quad (2)$$

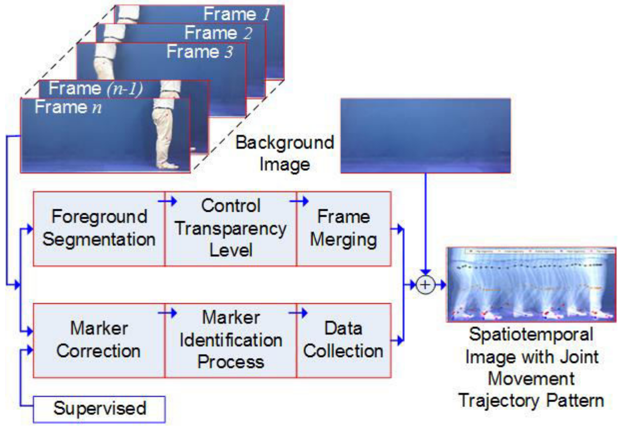

Figure-6. Complete block diagram of temporospatial image modelling and joint trajectory identification.

RESULT ANALYSIS

Figure-7 presents temporospatial image of 5 steps forward walking where initial step is made by Right Foot (R_f). Terminal step is also performed by R_f and gait process terminates when L_f and R_f comes at rest. First two steps and last two steps are involved in Gait Initiation (GI) and Gait Termination (GT) of walking. During GI, acceleration increases to normal speed and during GT, deceleration is clearly identical by overlapping regions. A gait cycle is defined by heel contact to next heel contact of same foot. Stride length is shown from heel position to heel position (or toe to toe position) of same foot. A step length is heel distance between two feet on sagittal plane of walking. Table-1 presents other properties of the gait.

ARPN Journal of Engineering and Applied Sciences

www.arpnjournals.com

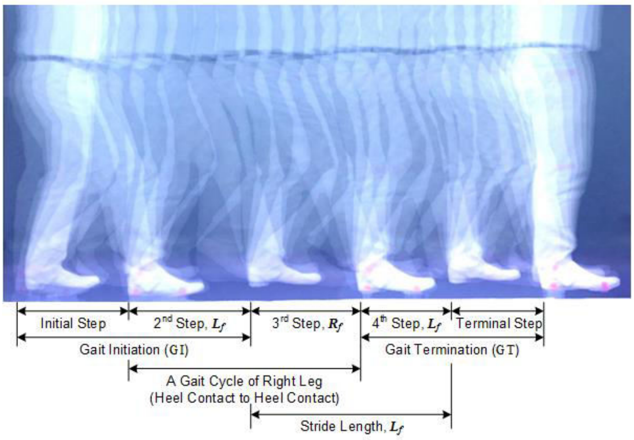

Figure-7. Spatiotemporal representation of five steps walking gait from Gait Initiation (GI) to Gait Termination (GT). Here, L_f and R_f are representing Left Foot and Right Foot respectively.

Figure-8 shows trajectory patterns of five significant points of human lower torso, Right Leg, on temporospatial image. Acceleration and deceleration of movements are clearly visible at the beginning and the end of gait, representing GI and GT. Knee decelerates from heel contact to mid-stance and accelerates again from mid-stance to toe off. During swing phase, knee presents comparatively higher speed of movement. Ankle, Heel, and Toe points also presents highest speeds during swing phase. Motion-rest for these three points occurs in between deceleration and acceleration while foot is in full contact with ground. Figure-9 provides a different view of movement patterns for all five significant positions where motion trajectories are presented based on time.

Table-1. Identifications of gait properties.

Gait Properties	Calculations	Values
Steps (Stp)	Measured	$Stp = 5$
Distance traveled (D)	Measured	$D \approx 200\ cm$
Time taken (T)	Measured	$T \approx 3000\ ms$
Walking speed (Sp)	$Sp = {}^{D}/_{T}$	$Sp \approx 0.67\ m\ s^{-1} \approx 2.40\ km\ h^{-1}$
Avg. step length (l_{stp})	$l_{stp} = {}^{D}/_{Stp}$	$l_{stp} \approx 40\ cm$
Avg. stride length (l_{str})	$l_{str} = l_{stp} * 2$	$l_{str} \approx 80\ cm$
Steps per minutes ($StpPerMin$)	$StpPerMin = {}^{Stp}/_{T}$	$StpPerMin \approx 100\ Stp\ min^{-1}$
Gait cycle (G_{cyc})	$G_{cyc} = {}^{T}/_{Stp} * 2$	$G_{cyc} \approx 1.2\ sec$

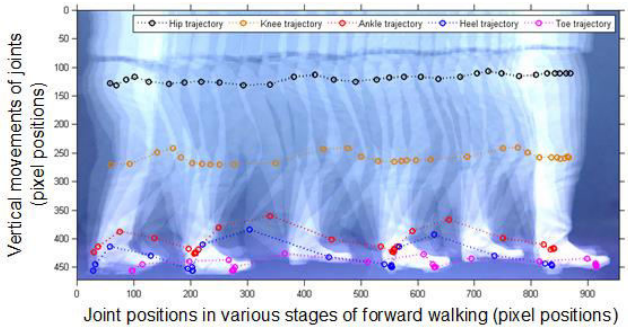

Figure-8. Joint position trajectories on spatiotemporal image of walking.

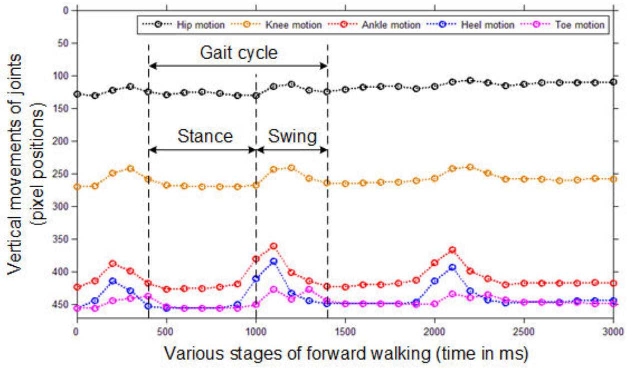

Figure-9. Joint position trajectories with respect to time in millisecond (ms).

According to Figure-9, duration of a gait cycle is identified as, $G_{cyc} \approx 1.2\ sec \approx 1.0\ sec$ ($T = 400\ ms$ to $T = 1400\ ms$, heel contact to heel contact). Within this time, stance phase occupies almost 60% of gait cycle, ($T = 400\ ms$ to $T = 1000\ ms$, heel contact to toe off. Swing phase continues about 40% of gait cycle, (from toe off to heel contact, $T = 1000\ ms$ to $T = 1400\ ms$). Figure-10 illustrates spatiotemporal pattern of right leg with stance and swing phase indications for walking gait.

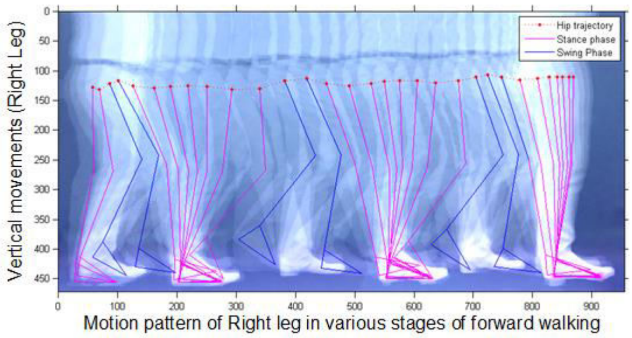

Figure-10. Presentation of spatiotemporal motion pattern of right leg in forward walking.

Figure-11 presents a conceptual model of human right leg focusing on three joint angles, Hip (θ_{Hp}), Knee

ARPN Journal of Engineering and Applied Sciences

(θ_{Kn}), and Ankle (θ_{An}). For this model, pelvis is always considered as upright position. Changing patterns of these three joint angles with respect to time variations are demonstrated in Figure-12.

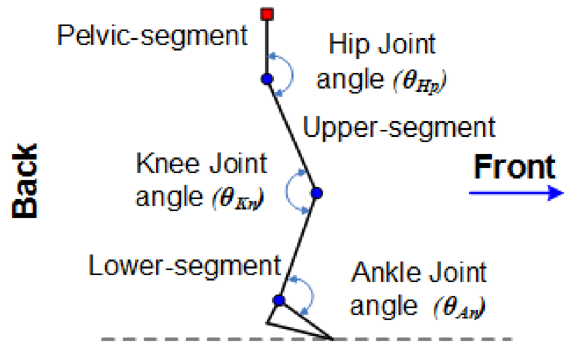

Figure-11. Conceptual model and joint angle indication of human lower limb (Right leg).

Figure-12 also exemplifies angular behaviour of three joints within a gait cycle, heel contact to successive heel contact. During stance phase (heel contact to toe off), ankle joint continues in decreasing fashion, hip joint angle keeps rising, and knee joint angle shows small deviation. At the beginning of swing phase (toe-off), both hip and knee joint reflect sudden fall in angle values while ankle shows sudden rising pattern. This behaviour of ankle joint is almost stable with some small deviation during swing phase. On the other hand, hip joint angle drops a little and begins gradual increasing manner while knee joint shows abrupt change in fall and rise of angle values.

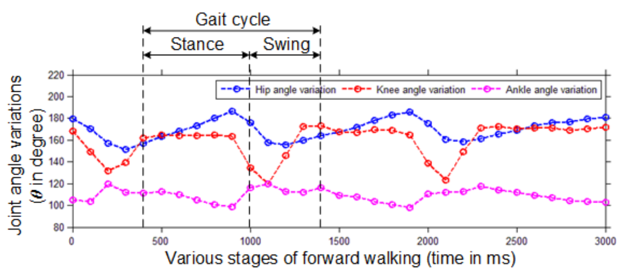

Figure-12. Joint angle variations of right leg in various stages of forward walking.

CONCLUSIONS

This project mainly investigates walking gait characteristics through 2D image analysis and presents behaviour patterns of walking gait from various points of view. The paper also represents image processing strategy in spatiotemporal image modelling, identification of marker points, and feature extraction. For this study, a single camera is used to capture lateral movements of forward walking, focusing on lower limbs especially on right leg. The subject performs five steps walking with initiation and termination of gait. To reduce the processing complexities, the setup of the experimental environment is designed with a single camera and a single-color background. Possible application of this study could be, human gait analysis, automatic gait recognition, and person identification.

ACKNOWLEDGEMENT

Authors would like to express their gratitude to the Ministry of Higher Education (MOHE), Malaysia, in funding the project through Fundamental Research Grant Scheme (FRGS).

REFERENCES

[1] Goffredo M., Seely R. D., Carter J. N. and Nixon M. S., 2008. Markerless view independent gait analysis with self-camera calibration. Proceedings of IEEE Conference on Automatic Face Gesture Recognition, 2008, pp. 1-6.

[2] E. F. A. Mashagba, F. F. A. Mashagba, M. O. Nassar, 2014. Simple and Efficient Marker-Based Approach in Human Gait Analysis Using Gaussian Mixture Model. Australian Journal of Basic and Applied Sciences, 8(1) January 2014, pp. 137- 147.

[3] Bilal S., Akmeliawati R., Salami M. J. E., Shafie A. A., 2011. Vision-based Hand Posture Detection and Recognition for Sign Language-A study. 4th International Conference on Mechatronics (ICOM), 17-19 May, Kuala Lumpur, Malaysia, pp. 1-6.

[4] D. A. Winter. 2009. Biomechanics and Motor Control of Human Movement. Chapter 3, Kinematics. Fourth Edition, Wiley, John Wiley and Sons, INC. 2009, pp. 45-81.

[5] Saboune J. and Charpillet F. 2005. Markerless Human Motion Capture for Gait Analysis. Proceedings of the 3rd European medical and biological engineering conference 2005, Prague.

[6] Rosenhahn B., Kersting U. G., Smith A. W., Gurney J. K., Brox T. and Klette R. 2005. A System for Marker-Less Human Motion Estimation. Proceedings of 27th DAGM Symposium, Vienna, Austria, August 31 - September 2, 2005, pp. 230-237.

[7] O. Rashid, A. Al-Hamadi, A. Panning, and B. Michaelis, 2009. Posture Recognition using Combined Statistical and Geometrical Feature Vectors based on SVM. World Academy of Science, Engineering and Technology, 56, pp. 590-597.

[8] R. Tranberg, 2010. Analysis of body motions based on optical markers, Accuracy, error analysis and clinical applications. University of Gothenburg, Göteborg, 2010.

[9] Hafiz F., Shafie A. A., Khalifa O., Ali M. H. 2010. Foreground segmentation-based human detection with shadow removal. 2010 International Conference on Computer and Communication Engineering (ICCCE), 11-13 May 2010, pp. 1-6.

[10] Jeevan M., Jain N., Hanmandlu M., and Chetty G. 2013. Gait Recognition Based on Gait Pal and Pal Entropy Image. 20th IEEE International Conference on Image Processing (ICIP), 15-18 Sept. 2013, pp. 4195-4199.